Nanoscale c1nr10176e

PAPER

1

Low temperature solution-phase growth of ZnSe and ZnSe/CdSe core/shell nanowires

Nattasamon Petchsang, Liubov Shapoval, Felix Vietmeyer, Yanghai Yu, Jose H. Hodak, I-Ming Tang, Thomas H. Kosel and Masaru Kuno*

High quality ZnSe nanowires (NWs) and complementary ZnSe/CdSe core/shell species have been synthesized using solution–liquid–solid (SLS) growth.

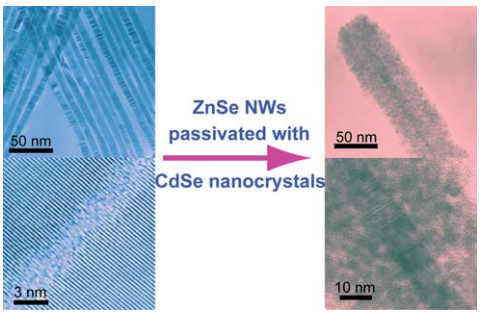

Please check this proof carefully. **Our staff will not read it in detail after you have returned it**.

Translation errors between word-processor files and typesetting systems can occur so the whole proof needs to be read. Please pay particular attention to: tabulated material; equations; numerical data; figures and graphics; and references. If you have not already indicated the corresponding author(s) please mark their name(s) with an asterisk. Please e-mail a list of corrections or the PDF with electronic notes attached – do not change the text within the PDF file or send a revised manuscript.

Please bear in mind that minor layout improvements, e.g. in line breaking, table widths and graphic placement, are routinely applied to the final version.

We will publish articles on the web as soon as possible after receiving your corrections; no late corrections will be made.

Please return your **final** corrections, where possible within **48 hours** of receipt by e-mail to: nanoscale@rsc.org

Reprints—Electronic (PDF) reprints will be provided free of charge to the corresponding author. Enquiries about purchasing paper reprints should be addressed via: http://www.rsc.org/publishing/journals/guidelines/paperreprints/. Costs for reprints are below:

Reprint costs

No of pages	Cost (per 50 copies)	
	First	Each additional
2–4	£225	£125
5–8	£350	£240
9–20	£675	£550
21–40	£1250	£975
>40	£1850	£1550

Cost for including cover of journal issue:
£55 per 50 copies

Nanoscale

Dynamic Article Links

Cite this: DOI: 10.1039/c1nr10176e

www.rsc.org/nanoscale

PAPER

Low temperature solution-phase growth of ZnSe and ZnSe/CdSe core/shell nanowires†

Nattasamon Petchsang,[abd] Liubov Shapoval,[c] Felix Vietmeyer,[d] Yanghai Yu,[e] Jose H. Hodak,[f] I-Ming Tang,[ab] Thomas H. Kosel[g] and Masaru Kuno*[d]

Received 15th February 2011, Accepted 30th April 2011
DOI: 10.1039/c1nr10176e

High quality ZnSe nanowires (NWs) and complementary ZnSe/CdSe core/shell species have been synthesized using a recently developed solution–liquid–solid (SLS) growth technique. In particular, bismuth salts as opposed to pre-synthesized Bi or Au/Bi nanoparticles have been used to grow NWs at low temperatures in solution. Resulting wires are characterized using transmission electron microscopy and possess mean ensemble diameters between 15 and 28 nm with accompanying lengths ranging from 4–10 μm. Subsequent solution-based overcoating chemistry results in ZnSe wires covered with CdSe nanocrystals. By varying the shell's growth time, different thicknesses can be obtained and range from 8 to 21 nm. More interestingly, the mean constituent CdSe nanocrystal diameter can be varied and results in size-dependent shell emission spectra.

Introduction

Bulk zinc selenide is an interesting material from an applications standpoint. It emits blue-green light, which can be used to make devices such as blue/green light emitting diodes[1] and blue lasers.[2] As a consequence, it has been extensively studied over the last few decades with the intent of improving its growth to minimize defects that limit its photo- and electro-luminescence efficiencies. Ref. 3 and 4 review these developments.

ZnSe NWs are also interesting from a basic science standpoint. Like ZnO (bulk exciton binding energy of 39 meV),[5] ZnSe possesses a relatively large bulk exciton binding energy on the order of 24 meV.[5] For comparison purposes, the bulk binding energy of GaAs is 5 meV[5] while that of CdSe is 14 meV.[5] When coupled to potential dielectric contrast effects,[6] excitonic behavior in ZnSe NWs may be prominent, even at room temperature.

Recent studies have focused on synthesizing nanostructured ZnSe. This has led to the development of colloidal ZnSe quantum dots (QDs)[7] as well as ZnSe nanowires (NWs). The synthesis of the latter exploits recent advances in the growth of one-dimensional (1D) nanostructures. Namely, ZnSe NWs have been grown using hard templates,[8] vapor–liquid–solid (VLS) growth[9–11] and molecular beam epitaxy (MBE).[12] Alternative solution-based approaches have also been explored and involve significantly lower growth temperatures. These techniques include solvothermal syntheses,[13] oriented attachment[14] and solution–liquid–solid (SLS) NW growth.[15,16]

In this study, we exploit the latter SLS growth strategy to synthesize ZnSe NWs. The approach bootstraps onto recent developments we have made, using $BiCl_3$, as opposed to pre-made Bi[16–19] or Au/Bi nanoparticles (NPs),[20] to induce NW growth.[21] What results are crystalline ZnSe NWs with mean diameters that range from 15 nm ($\sigma = 2$ nm) to 28 nm ($\sigma = 5$ nm). Resulting NWs are then overcoated with a CdSe shell, creating potential (inverted) Type-I heterojunctions.

In this regard, very few NW overcoating studies exist.[19,22–24] Within the realm of colloidal QDs, such overcoating approaches have been instrumental in improving the usefulness of nanocrystals for various applications, ranging from biological labeling to lasing studies. Similar advances with solution-based NWs may likewise usher in potential applications.

Experimental

Materials

Zinc stearate (~86%), 1-octadecene (90%), 1-hexadecylamine (90%), dodecylamine (98%), phenyl ether (99%), bismuth(III)

[a]Mahidol University, Department of Physics, Rama 6, Bangkok, Thailand 10400
[b]ThEP, Commission of Higher Education, Thailand Ministry of Education, Bangkok, Thailand 10400
[c]Herzen State Pedagogical University of Russia, Chemistry Department, Moyka emb. 48, Saint-Petersburg, Russia 191186
[d]University of Notre Dame, Department of Chemistry and Biochemistry, Notre Dame, IN, 46556, USA. E-mail: mkuno@nd.edu; Fax: +1 574-631-6652; Tel: +1 574-631-0494
[e]Department of Chemistry, University of Wisconsin-Madison, Madison, WI, 53705, USA
[f]DQIAyQF/INQUIMAE—FCEN Universidad de Buenos Aires Ciudad Universitaria, Pab. 2, piso 3, C1428EHA Buenos Aires, Argentina
[g]University of Notre Dame, Department of Electrical Engineering, Notre Dame, IN, 46556, USA

† Electronic supplementary information (ESI) available. See DOI: 10.1039/c1nr10176e

chloride (98%), cadmium acetate dihydrate (98%) and selenium powder (99.5%) were purchased from Acros. ZnSe powder (99.99%, 5 micron, metals basis), squalane (99%), tri-octylphosphine (TOP, 90%) and tri-*n*-octylphosphine oxide (TOPO, 99%) were purchased from Aldrich. Additional TOPO 99% and TOPO 90% were purchased from Strem Chemicals. Oleylamine (70%) and *n*-octyl ether (>95.0%) were purchased from TCI. Methanol, acetone, and toluene were purchased from Fisher Scientific and VWR. Unless otherwise noted, all chemicals were used as received. 1 M TOPSe was prepared under nitrogen in a glovebox by mixing Se powder (0.39 g, 5 mmol) with TOP (5 mL, 11.2 mmol). The solution was then left to stir overnight to complete the reaction. Bi catalyst was freshly prepared prior to each NW synthesis by diluting 23.3 mg (74 μmol) $BiCl_3$ in 4.0 mL of acetone. The solution was further diluted to 1.68 mM and 60 μL of it was used in subsequent reactions.

ZnSe NW synthesis

A representative preparation using a 2 : 1 Zn-to-Se mole ratio is described. More details about the ZnSe NW synthesis, including a discussion of the parameter space explored, can be found in the ESI†.

In a three neck flask connected to a Schlenk line, TOPO (2.5 g, 6.5 mmol, 99%) was mixed with zinc stearate (30 mg, 47.5 μmol). The mixture was then dried and degassed at 100 °C for 1 hour. Once complete, the vessel was backfilled with N_2 and the temperature was raised to 310 °C. In tandem, TOPSe (25 μL, 25 μmol), TOP (0.2 mL, 0.45 mmol) and $BiCl_3$ (60 μL acetone solution, 0.1 μmol) were mixed together in a syringe. When the temperature of the growth mixture stabilized, the solution was injected into the three neck flask, yielding a gradual color change from clear to yellow.

Following the injection, the resulting reaction mixture was heated at temperatures between 304 and 307 °C for 30 minutes. Afterwards, it was allowed to cool to 70 °C, whereupon 10 mL of toluene was introduced to prevent TOPO from solidifying. Resulting NWs were precipitated using an excess of methanol (~15 mL) and were recovered by centrifuging the suspension, discarding the supernatant. A 1 : 1.5 mixture of toluene : methanol (by volume) was then added to remove excess surfactant from the NW precipitate. The suspension was again centrifuged and the product was recovered. This washing procedure was repeated two more times whereupon the recovered NWs were stored in toluene. For overcoating reactions, the above synthesis was scaled up by a factor of three.

Pyridine stripping procedure

An aliquot of the ZnSe NW stock was centrifuged to isolate the wires. Neat pyridine was subsequently added to resuspend the recovered material. The resulting mixture was heated at 60 °C for 15 min whereupon NWs were precipitated using hexane. The product was re-dispersed in fresh pyridine and the heating/precipitation steps were repeated two more times. To prevent any adverse effects caused by prolonged exposure to pyridine, the final "stripped" ZnSe NWs were stored in toluene and were then used in the core/shell reactions described below. The NW concentration was calculated by assuming mean diameters measured by transmission electron microscopy (TEM), a representative length of 6 μm and molar extinction coefficients, obtained using model expressions for NW absorption cross-sections.[25–27] More details about these estimates can be found in the ESI†.

ZnSe/CdSe core/shell NW synthesis

Pyridine-stripped ZnSe NWs in toluene (0.75 mL, ~4.6×10^{-14} mol) and cadmium acetate (0.1 g, 375 μmol) were added to TOPO 99% (1 g, 2.6 mmol) in a three neck flask connected to a Schlenk line. The mixture was then dried and degassed for 40 minutes at 100 °C to completely remove the toluene. Once complete, the vessel was backfilled with N_2 and the temperature was raised to 140 °C to decompose the cadmium precursor. After this, the temperature was lowered to 110–130 °C whereupon a solution of 1 M TOPSe (100 μL, 100 μmol) was injected into the three neck flask. The reaction time was varied between 3 and 30 minutes (as described in the main text) and was accompanied by a color change from yellow to red. Finally, the mixture was cooled to 70 °C whereupon toluene was added to prevent TOPO from solidifying.

ZnSe/CdSe core/shell NWs were recovered by centrifuging the suspension and discarding the supernatant which contained unwanted CdSe QD byproducts. Toluene was then added to the precipitate to wash the wires of excess surfactant. The suspension was centrifuged and the product was recovered. This washing procedure was repeated three more times whereupon the isolated ZnSe/CdSe core/shell NWs were stored in toluene.

Characterization

Both ZnSe and ZnSe/CdSe NWs were characterized using TEM. Dilute suspensions of wires in toluene were dropped onto 200 mesh ultrathin carbon TEM grids (Ladd). Survey images were acquired using a JEOL 100SX instrument. Low and high resolution TEM micrographs were taken with a JEOL 2010 TEM operating at 200 kV. Scanning transmission electron microscopy (STEM) was performed using a Titan 80–300 TEM (FEI). NW elemental analyses were conducted using an energy-dispersive X-ray spectroscopy (EDXS) attachment to the JEOL 2010 microscope (Thermo Scientific) with ZnSe powder as a standard. X-Ray diffraction patterns were acquired using a Bruker D8 Discover powder diffractometer (Cu Kα source). Ensemble extinction and emission spectra of NW samples were recorded with a Cary 50 Bio spectrometer and a commercial fluorimeter (Horiba).

Results and discussion

To date, a number of vapor-phase[9–12] and solution-phase[8,13–17] approaches exist for synthesizing ZnSe NWs. There are also recent SLS approaches,[28,29] which employ premade Bi nanoparticles to induce the asymmetric growth of ZnSe NWs.[15,16] With the notable exception of oriented attachment,[14] all prior syntheses produce wires with diameters ranging from 12–100 nm and with lengths exceeding 10 μm.

In the case of solution-based reactions, specifically SLS reactions, resulting wires are highly crystalline and show lattice fringes in corresponding TEM micrographs. This illustrates that,

ART ■ C1NR10176E

despite the low growth temperatures typical of these preparations, high quality NWs can be made. Many of these samples also exhibit instances of twinning as well as zinc blende (ZB) and wurtzite (W) phase admixtures. Both phenomena have previously been seen in other II–VI[30,31] as well as III–V NWs[32] and occur due to the low energy difference between the phases in these materials.

In the current study, we first demonstrate the synthesis of high quality ZnSe NWs using $BiCl_3$ as a catalyst precursor. Low and high resolution TEM images of representative wires are shown in Fig. 1. Additional images can be found in the ESI† (Fig. S1†). In the specific case shown (Fig. 1), the average NW diameter is $d = 22$ nm ($\sigma = 3$ nm) [sample size = 108]. Corresponding intrawire diameter variations are approximately 5% ($\sigma = 1.1$ nm) [sample size = 20] and corroborate the above low resolution micrographs, which suggest highly uniform NWs.

By varying reaction parameters such as the metal-to-chalcogen precursor stoichiometry, the amount of Bi catalyst used and the overall injection/growth temperatures, we find that ZnSe NWs with diameters ranging from $d = 15$ to $d = 28$ nm can be synthesized. A detailed discussion of the parameter space explored can be found in the ESI†. Under optimized conditions, accompanying NW lengths are on the order of 10 μm and yield aspect ratios close to 500. With the exception of CdSe NWs,[33] no length control has been reported in SLS preparations to date.

Fig. 2 shows additional high resolution TEM (HRTEM) images of ⟨110⟩-oriented NW samples and reveals that the wires also possess ZnSe ZB/W phase admixtures. Evidence for this can be seen in the HRTEM images since when samples with ⟨111⟩ growth directions are viewed down the ⟨110⟩ zone axis, characteristic "zig-zag" lattice fringes are apparent. This highlights both the ZB and W phases present within them.[30] More HRTEM

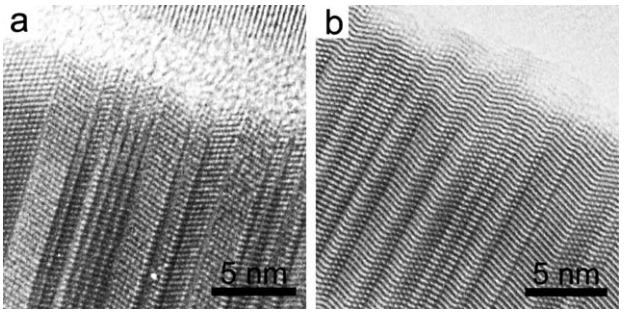

Fig. 2 (a and b) HRTEM images of ⟨110⟩-oriented ZnSe NWs, showing evidence of twinning as well as ZB/W phase admixtures.

micrographs can be found in the ESI† (Fig. S2†). Ensemble powder X-ray diffraction patterns corroborate this conclusion, showing both ZB and W reflections (ESI†, Fig. S3†).

The ZnSe NWs in our synthesis form *via* a SLS growth mechanism whereby $BiCl_3$ introduced into the reaction mixture produces Bi NPs.[21] These nanocrystals, in turn, promote NW crystallization.[28,29] Evidence for this growth mechanism centers primarily on the existence of catalyst nanoparticles located at NW ends. This is shown in Fig. 3 where high resolution TEM images show examples of attached Bi particles. Accompanying insets show the NPs at lower magnification.

An important property of low dimensional materials is their surface. This is because the abrupt termination of nanostructures means that dangling bonds and other defects exist, which strongly influence their optical and electrical properties. As a consequence, learning to control this interface is key to eventually using these nanostructures in applications. It is also crucial to unraveling their underlying photophysics.

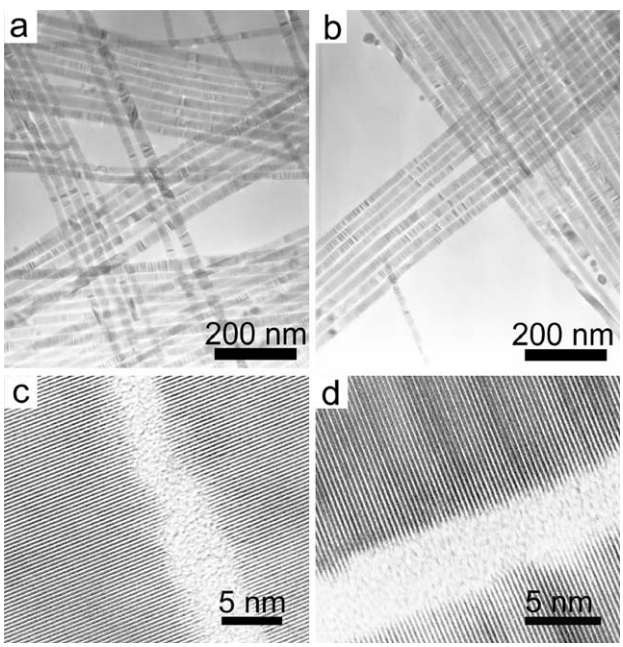

Fig. 1 Low (a and b) and high-resolution (c and d) TEM images of ZnSe NWs produced under the conditions described in the main text. High resolution TEM images of ZnSe NWs, showing {111} lattice planes normal to their ⟨111⟩ growth axes.

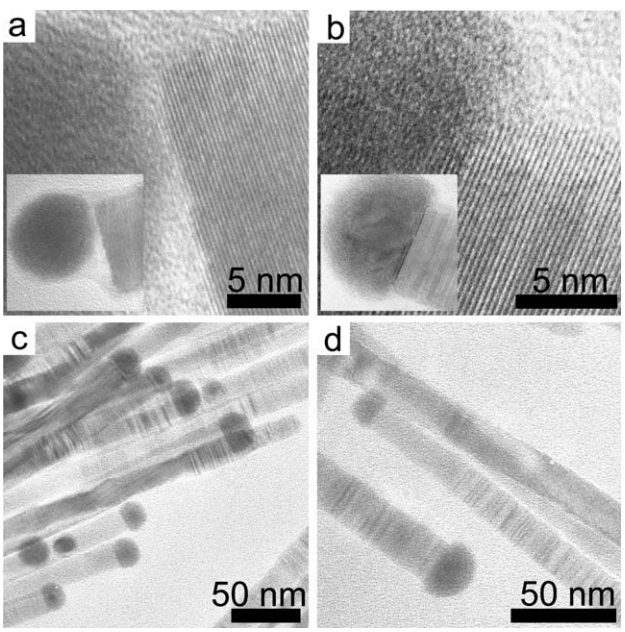

Fig. 3 (a–d) High and low resolution TEM images of Bi NPs attached to NW ends. The insets show the catalyst/NW junction at lower magnification.

Within the realm of colloidal QDs, the ability to coat them with different semiconductor shells has led to dramatic improvements in their optical properties.[34–37] As illustrations, CdSe QDs can now be passivated with ZnS, CdS, and ZnSe. All provide barriers for carriers in the nanocrystal core. As a consequence, ensemble emission quantum yields now routinely exceed 30%. Such overcoating strategies have also led to the suppression of interesting but unwanted phenomena such as fluorescence intermittency.[38,39]

By contrast, analogous overcoating investigations on solution-based semiconductor nanowires are lacking. We know of only a handful of studies that describe the surface coating of NWs using chemical means. Results from these experiments have been decidedly mixed. In this regard, early attempts have demonstrated that VLS-grown InP wires can be coated with CdS using wet chemistry.[22] However, emission quantum yields were seen to decrease due to the introduction of additional defects during the coating procedure. More recent studies have shown that CdSe (CdS) NWs can be passivated with CdS and ZnTe (CdSe).[24] Enhancements in the emission quantum yield were possibly seen though a definitive conclusion is complicated by the need to first strip the NWs of their native surface-passivating agent. This introduces additional surface defects prior to the overcoating step and makes any assessment of shell-induced emission enhancements ambiguous.

PbSe NWs have also been passivated with PbS and PbTe using a solution-based successive ion layer adsorption and reaction (SILAR) approach. However no quantum yields were reported.[24] Along these lines, Mews *et al.* have recently coated CdSe NWs with CdS using an analogous approach.[19] In this latter study, the emission quantum yield increased, though ultimately remained below 1% (~0.2%). The current ZnSe study therefore adds to a growing body of knowledge about solution-based NW overcoating strategies and illustrates an approach for producing controlled shell thicknesses with sizable (shell) emission quantum yields.

ZnSe NWs are coated with CdSe by first exposing pre-synthesized/stripped wires to a Cd precursor at moderate temperatures. This is followed by the injection of TOPSe to initiate shell growth. More information about the procedure can be found in the Experimental section. Fig. 4 shows TEM images of resulting core/shell NWs with an average core diameter of $d = 16$ nm ($\sigma = 3$ nm) [sample size = 16] and a shell thickness of 12 nm ($\sigma = 3$ nm) [sample size = 31].

Interestingly, the developed procedure results in uniform NW coatings. Specifically, for the representative sample shown in Fig. 4, an examination of resulting core/shell diameters yields intrawire diameter variations of 7% ($\sigma = 3$ nm). Accompanying lengths are on the order of 10 μm and reveal that NW core lengths are preserved during the coating procedure.

HRTEM images of overcoated wires are shown in Fig. 5(a and b) where lattice fringes from the core are clearly visible. The surrounding, lighter contrast, shell appears polycrystalline as evidenced by fringes from smaller grains, oriented in different directions. Additional high resolution TEM micrographs of other overcoated wires can be found in the ESI† (Fig. S4†).

A nice feature of the current overcoating approach is the ability to control the resulting shell thickness. Namely, by varying the shell growth time after the injection of the chalogen

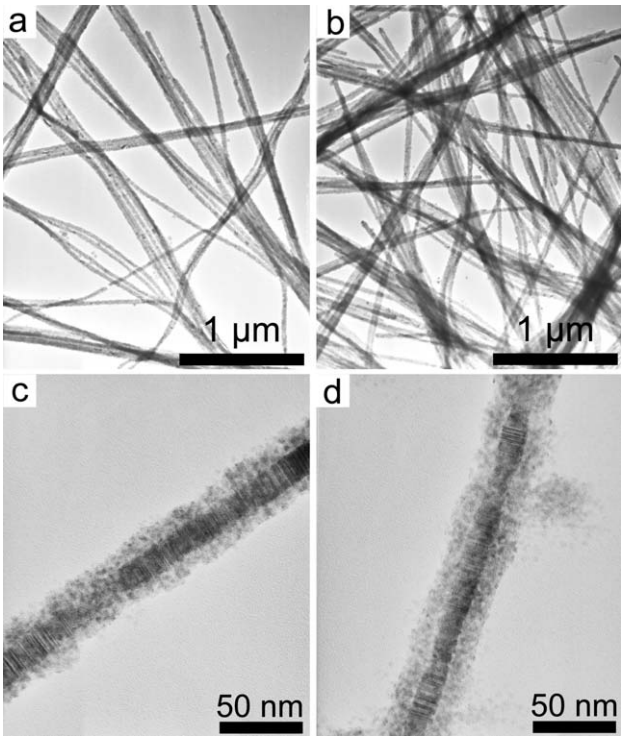

Fig. 4 (a and b) Low and (c and d) high resolution TEM images of ZnSe/CdSe core/shell NWs with a core diameter of $d = 16$ nm ($\sigma = 3$ nm) and a shell thickness of 12 nm ($\sigma = 3$ nm).

precursor, CdSe shell thicknesses up to 21 nm can be produced on the same core wires. This is illustrated in Fig. 6(a–d) where $d = 15$ nm ($\sigma = 2$ nm) ZnSe NWs [sample size = 35] have been coated with 8 nm ($\sigma = 3$ nm) [sample size = 27] (Fig. 6a), 9 nm ($\sigma = 3$ nm) [sample size = 28] (Fig. 6b), 18 nm ($\sigma = 3$ nm) [sample size = 27] (Fig. 6c), and 21 nm ($\sigma = 5$ nm) [sample size = 20] (Fig. 6d) thick CdSe shells by simply varying the shell growth time from 3 minutes to 30 minutes. Additional details about the overcoating procedure and the parameter space explored to optimize these reactions can be found in the ESI†.

Energy-dispersive X-ray spectroscopy (EDXS) analyses of small ensembles (sample size <10 NWs) were performed on both core and core/shell NWs to confirm their composition. EDXS spectra of core NWs show nearly stoichiometric ZnSe wires

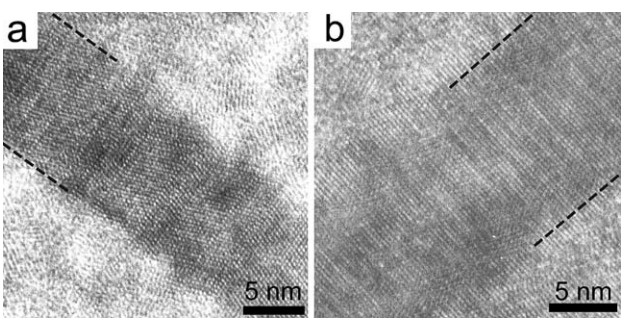

Fig. 5 (a and b) HRTEM images of ZnSe/CdSe core/shell NWs that illustrate the core's lattice fringes and those of the surrounding polycrystalline shell.

ART ■ C1NR10176E

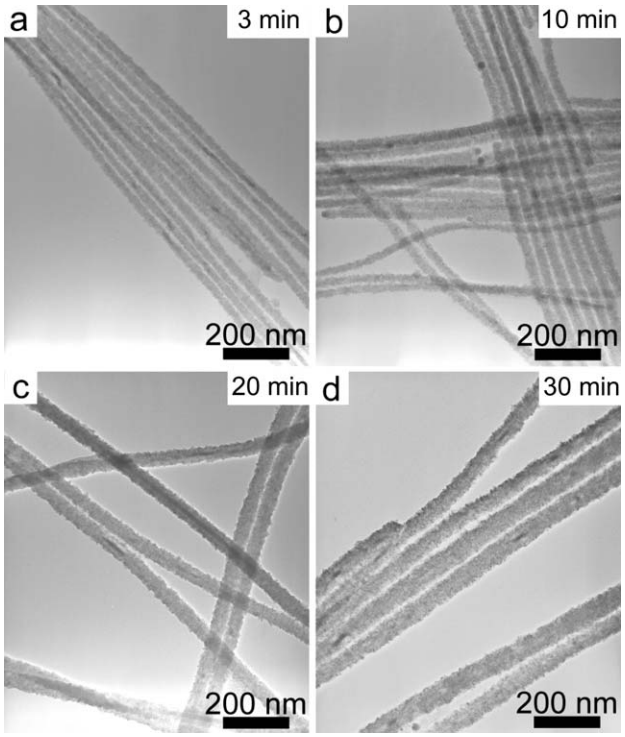

Fig. 6 TEM images of ZnSe/CdSe core/shell NWs with a core diameter of $d = 15$ nm ($\sigma = 2$ nm) and with different shell thicknesses of (a) 8, (b) 9, (c) 18, and (d) 21 nm. Variable shell thicknesses were obtained by varying the shell growth time from 3 minutes to 30 minutes.

(*e.g.* Zn : Se 49 : 51% or ~1 : 1). For the core/shell species, EDXS results of entire NWs show that an approximate 1 : 1 metal to selenium ratio is maintained (*e.g.* Zn 10%, Cd 46%, and Se 44%). EDXS spectra for both bare and coated NWs are shown in the ESI† (Fig. S5 and S6†).

Interestingly, the mean CdSe nanocrystal size composing the coating appears to correlate with the shell's overall thickness. This is evident when taking photoluminescence (PL) spectra of resulting core/shell wires. Namely, emission from the CdSe shell can be seen with a peak wavelength that varies with its thickness. This likely arises from size-dependent confinement effects that stem from systematic variations of the underlying (CdSe) nanocrystal size.[40]

Before discussing this observation in more detail, Fig. 7 shows a representative extinction spectrum of uncoated ZnSe NWs (dash dot-dot line). An apparent absorption edge can be seen at 2.76 eV (450 nm), which agrees well with both the 2.7 eV (459 nm) and 2.8 eV (443 nm) bulk band gaps of ZB and W ZnSe.[41] No apparent confinement effects are seen in any of the ZnSe NWs we have made. This is consistent with mean ensemble diameters between 15 and 28 nm that are larger than twice ZnSe's bulk exciton Bohr radius ($a_B \approx 5.4$ nm).[41] Note that an emission spectrum of core ZnSe NWs could not be obtained at the ensemble level due to their low quantum yields.

Fig. 7 also shows representative extinction (solid blue line) and emission spectra (dashed red line) of ZnSe/CdSe core/shell NWs synthesized at 110 °C for 30 minutes. The particular coating reaction highlighted results in a relatively thick 21 nm shell. Two shoulders exist in the core/shell extinction spectrum, the first

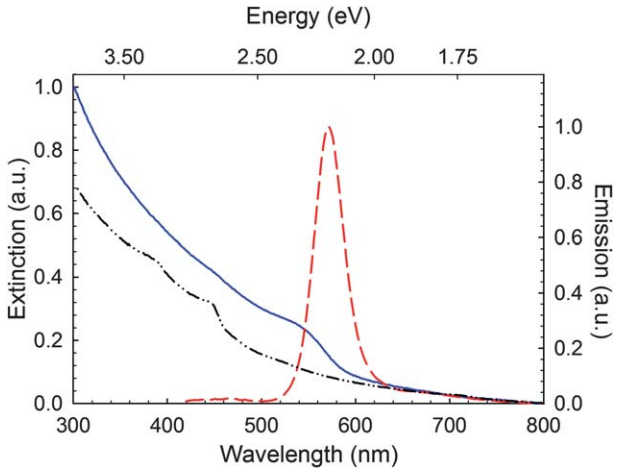

Fig. 7 Extinction spectra of ZnSe (black dash dot-dot line) and ZnSe/CdSe core/shell NWs (blue solid line). Also shown is the emission spectrum of core/shell NWs (red dashed line).

occurs at 450 nm (2.76 eV) while the second appears at 545 nm (2.28 eV). By comparing this spectrum to that of uncoated NWs, we assign the higher energy feature to absorption by the ZnSe core while the second is likely due to absorption by the CdSe shell. The core/shell sample's corresponding photoluminescence peaks at 570 nm (2.18 eV) and suggests that its emission is dominated by shell contributions since the emission maximum occurs far to the red of ZnSe's bulk band gap. Furthermore, it occurs at energies larger than CdSe's bulk band gap, implying that the shell is composed of confined CdSe grains, as first suggested by the HRTEM micrographs in Fig. 5.

What is interesting then is that the shell's emission wavelength varies when its thickness changes. This can be seen in Fig. 8 where both the extinction and photoluminescence of core/shell ensembles have been plotted for different growth times between 3 minutes and 30 minutes. Associated with each pair of spectra are different shell thicknesses. Namely, in the 3 minute case the shell thickness is 8 nm while it is 21 nm in the 30 minute case. Intermediate values can be found in between as denoted in the figure. Redshifts in the absorption and emission therefore occur with increasing time and indicate that the average CdSe nanocrystal size grows along with the shell's thickness. Note that a broad emission peak, centered at ~680 nm, also exists at early times in Fig. 8. We suggest that it arises from CdSe gap states. At longer times, this peak does not disappear. Instead, it is masked by the much stronger CdSe band edge emission.

It is well established that confined CdSe nanocrystals exhibit size-dependent absorption and emission spectra.[40] In tandem, there are now absorption and emission sizing curves[42] that allow us to estimate mean nanocrystal sizes based on their optical spectra. As a consequence, we can also estimate the effective size of the nanocrystalline grains, composing the coating, for varying shell thicknesses. Fig. S7 in the ESI† plots both the CdSe band edge absorption and emission wavelengths as a function of shell thickness along with the (effective) nanocrystal diameter, corresponding to these absorption and emission wavelengths. We find that mean nanocrystal diameters range from 3.1 nm to 4.0 nm and are associated with shell thicknesses between 8 and 21 nm. The average nanocrystal size is in fair agreement with a TEM

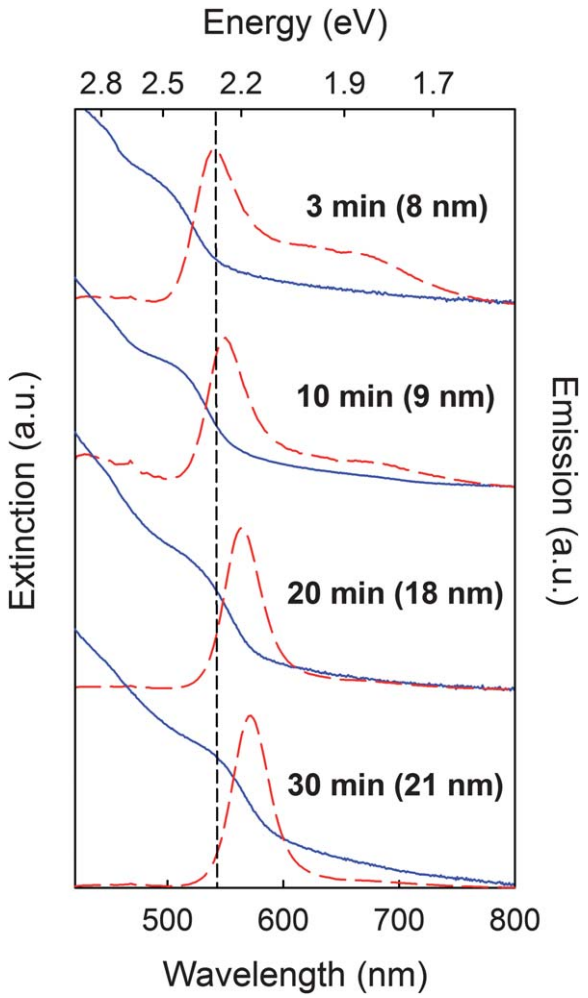

Fig. 8 Extinction (blue solid lines) and emission (red dashed lines) spectra of ZnSe/CdSe core/shell NWs with different shell thicknesses. The absorption and emission curves are not drawn to the same scale.

analysis of coated samples, which shows separate CdSe particles. A representative image can be found in the ESI† (Fig. S8†). Finally, although CdSe nanocrystals incorporated during early stages of the shell growth might be expected to be smaller than those attached at later times, the existence of a diameter gradient in the shell is difficult to prove by TEM because multiple nanocrystal layers exist simultaneously on the core nanowire surface. Cross sectional TEM experiments might address this issue and are therefore left for a future study.

We hypothesize that the size dependence of the nanocrystals forming the shell most likely originates from "free" CdSe QDs growing in solution adding to NW surfaces where they merge with existing (surface nucleated) CdSe grains. Provided the faster nucleation/growth kinetics of free CdSe particles over those on surfaces, this means that short duration overcoating reactions predominantly involve the addition of small nanocrystals whereas at longer times larger particles add to the shell. The end result is an apparent correlation between the overall shell thickness and the mean constituent nanocrystal size. This hypothesis is corroborated by photoluminescence studies where we have compared the spectral position of emission from unwanted "free" nanocrystals in solution to those attached to nanowire surfaces. We find that the PL of these unassociated nanocrystals exhibit systematic red-shifts relative to the emission of particles embedded in the shell (Fig. S9, ESI†). We interpret this as originating from the underlying difference in their average growth rates.

The proposed shell formation mechanism is further supported by Z-contrast STEM images of samples having 18 nm shell thicknesses. A representative image is shown in Fig. S10† where dark and bright spots correspond to intensity fluctuations that indicate variations of the shell thickness. In this regard, the significant surface roughness along the NW length appears to arise from the random process of CdSe nanocrystals attaching to the ZnSe core, consistent with the proposed hypothesis. By contrast, in the case where heterogenous nanocrystal nucleation occurs one might expect a much smoother shell to result.

Conclusion

High quality ZnSe NWs and corresponding ZnSe/CdSe core/shell species have been synthesized using solution–liquid–solid growth. The approach employs bismuth salts instead of pre-synthesized Bi nanoparticles to induce nanowire formation. What results are highly uniform ZnSe wires with diameters less than 28 nm and with lengths that exceed 10 μm. Subsequent overcoating reactions yield core/shell wires with uniform shell thicknesses that can be varied by simply altering the shell growth time. TEM microscopy indicates a coating that consists of CdSe nanocrystals. Subsequent photoluminescence experiments show strong emission from these CdSe particles. Interestingly, a correlation exists between the shell thickness and the mean constituent nanocrystal size. Namely, thinner shells appear to consist predominantly of smaller nanocrystals while thicker shells seem to have a significant fraction of larger particles. This can be seen through size-dependent shell emission spectra, tunable between 540 and 570 nm. The effect likely arises from independently growing CdSe nanocrystals adding to ZnSe NW surfaces during shell growth. The present study thus advances our ability to manipulate semiconductor nanowire interfaces and may ultimately aid future NW applications.

Acknowledgements

We thank the Notre Dame Strategic Research Initiative for funding this study. N.P. and I.M.T. thank the Thailand Research Fund through the Royal Golden Jubilee PhD Program (Grant No. PHD/0279/2549) as well as the Commission of Higher Education, Thailand Ministry of Education. L.S. thanks the Fulbright Foreign Student Program. M.K. also thanks the National Science Foundation CAREER program (CHE-0547784) and the Notre Dame Radiation Laboratory/Department of Energy, Office of Basic Energy Sciences for partial financial support and for use of their facilities. Masaru Kuno is a Cottrell Scholar of Research Corporation.

References

1 T. D. Thompson, *Semicond. Sci. Technol.*, 1991, **6**, 1015.
2 M. A. Haase, J. Qiu, J. M. DePuydt and H. Cheng, *Appl. Phys. Lett.*, 1991, **59**, 1272.

3 S. Guha, J. M. DePuydt, M. A. Haase, J. Qiu and H. Cheng, *Appl. Phys. Lett.*, 1993, **63**, 3107.
4 G. F. Neumark, *Mater. Sci. Eng., R*, 1997, **21**, 1.
5 J. Sun, L.-W. Wang and W. E. Buhro, *J. Am. Chem. Soc.*, 2008, **130**, 7997.
6 E. A. Muljarov, E. A. Zhukov, V. S. Dneprovskii and Y. Masumoto, *Phys. Rev. B: Condens. Matter Mater. Phys.*, 2000, **62**, 7420.
7 M. A. Hines and P. Guyot-Sionnest, *J. Phys. Chem. B*, 1988, **102**, 3655.
8 N. Kouklin, L. Menon, A. Z. Wong, D. W. Thompson, J. A. Woollam, P. F. Williams and S. Bandyopadhyay, *Appl. Phys. Lett.*, 2001, **79**, 4423.
9 U. Philipose, S. Yang, T. Xu and H. E. Ruda, *Appl. Phys. Lett.*, 2007, **90**, 063103.
10 X. T. Zhang, Z. Liu, K. M. Ip, Y. P. Leung, Q. Li and S. K. Hark, *J. Appl. Phys.*, 2004, **95**, 5752.
11 Y. Jiang, X.-M. Meng, W.-C. Yiu, J. Liu, J.-X. Ding, C.-S. Lee and S.-T. Lee, *J. Phys. Chem. B*, 2004, **108**, 2784.
12 Y. F. Chan, X. F. Duan, S. K. Chan, I. K. Sou, X. X. Zhang and N. Wang, *Appl. Phys. Lett.*, 2003, **83**, 2665.
13 J. Wang and Q. Yang, *Cryst. Growth Des.*, 2008, **8**, 660.
14 A. B. Panda, S. Acharya and S. Efrima, *Adv. Mater.*, 2005, **17**, 2471.
15 A. Dong, F. Wang, T. L. Daulton and W. E. Buhro, *Nano Lett.*, 2007, **7**, 1308.
16 D. D. Fanfair and B. A. Korgel, *Chem. Mater.*, 2007, **19**, 4943.
17 D. D. Fanfair and B. A. Korgel, *Cryst. Growth Des.*, 2005, **5**, 1971.
18 F. Wang and W. E. Buhro, *Small*, 2010, **6**, 573.
19 Z. Li, X. Ma, Q. Sun, Z. Wang, J. Liu, Z. Zhu, S. Z. Qiao, S. C. Smith, G. (Max) Lu and A. Mews, *Eur. J. Inorg. Chem.*, 2010, 4325.
20 J. W. Grebinski, K. L. Richter, J. Zhang, T. H. Kosel and M. Kuno, *J. Phys. Chem. B*, 2004, **108**, 9745.
21 J. Puthussery, T. H. Kosel and M. Kuno, *Small*, 2009, **5**, 1112.
22 Z. Zanolli, B. A. Wacaser, M.-E. Pistol, K. Deppert and L. Samuelson, *J. Phys.: Condens. Matter*, 2007, **19**, 295218.
23 J. A. Goebl, R. W. Black, J. Puthussery, J. Giblin, T. H. Kosel and M. Kuno, *J. Am. Chem. Soc.*, 2008, **130**, 14822.
24 T. Mokari, S. E. Habas, M. Zhang and P. Yang, *Angew. Chem.*, 2008, **120**, 5687.
25 J. Giblin, V. Protasenko and M. Kuno, *ACS Nano*, 2009, **3**, 1979.
26 J. Giblin and M. Kuno, *J. Phys. Chem. Lett.*, 2010, **1**, 3340.
27 V. Protasenko, D. Bacinello and M. Kuno, *J. Phys. Chem. B*, 2006, **110**, 25322.
28 M. Kuno, *Phys. Chem. Chem. Phys.*, 2008, **10**, 620.
29 F. Wang, A. Dong, J. Sun, R. Tang, H. Yu and W. E. Buhro, *Inorg. Chem.*, 2006, **45**, 7511.
30 J. W. Grebinski, K. L. Hull, J. Zhang, T. H. Kosel and M. Kuno, *Chem. Mater.*, 2004, **16**, 5260.
31 M. Kuno, O. Ahmad, V. Protasenko, D. Bacinello and T. H. Kosel, *Chem. Mater.*, 2006, **18**, 5722.
32 F. M. Davidson, D. C. Lee, D. D. Fanfair and B. A. Korgel, *J. Phys. Chem. C*, 2007, **111**, 2929.
33 Z. Li, O. Kurtulus, N. Fu, Z. Wang, A. Kornowski, U. Pietsch and A. Mews, *Adv. Funct. Mater.*, 2009, **19**, 3650.
34 M. A. Hines and P. Guyot-Sionnest, *J. Phys. Chem.*, 1996, **100**, 468.
35 B. O. Dabbousi, J. Rodriguez-Viejo, F. V. Mikulec, J. R. Heine, H. Mattoussi, R. Ober, K. F. Jensen and M. G. Bawendi, *J. Phys. Chem. B*, 1997, **101**, 9463.
36 X. Peng, M. C. Schlamp, A. V. Kadavanich and A. P. Alivisatos, *J. Am. Chem. Soc.*, 1997, **119**, 7019.
37 P. Reiss, J. Bleuse and A. Pron, *Nano Lett.*, 2002, **2**, 781.
38 M. Kuno, D. P. Fromm, H. F. Hamann, A. Gallagher and D. J. Nesbitt, *J. Chem. Phys.*, 2000, **112**, 3117.
39 M. Nirmal, B. O. Dabbousi, M. G. Bawendi, J. J. Macklin, K. Trautman, T. D. Harris and L. E. Brus, *Nature*, 1996, **383**, 802.
40 C. B. Murray, D. J. Norris and M. G. Bawendi, *J. Am. Chem. Soc.*, 1993, **115**, 8706.
41 *Optical Properties of Solids*, ed. M. Fox, Oxford University Press, Oxford, UK, 2001, p. 278, p. 78.
42 M. Kuno, *Band Edge Spectroscopy of CdSe Quantum Dots*, PhD thesis, Massachusetts Institute of Technology, Cambridge, MA, 1998.

Authors Queries

Journal: **NR**

Paper: **c1nr10176e**

Title: **Low temperature solution-phase growth of ZnSe and ZnSe/CdSe core/shell nanowires**

Editor's queries are marked like this... **1**, and for your convenience line numbers are inserted like this... 5

Query Reference	Query	Remarks
1	For your information: You can cite this article before you receive notification of the page numbers by using the following format: (authors), Nanoscale, (year), DOI: 10.1039/c1nr10176e.	